Special Effect of β-Cyclodextrin on the Aggregation Behavior of Mixed Cationic/Anionic Surfactant Systems

Lingxiang Jiang,[†] Manli Deng,[‡] Yilin Wang,*[,‡] Dehai Liang,[†] Yun Yan,[†] and Jianbin Huang*[,†]

Beijing National Laboratory for Molecular Sciences (BNLMS), State Key Laboratory for Structural Chemistry of Unstable and Stable Species, College of Chemistry and Molecular Engineering, Peking University, Beijing 100871, People's Republic of China, and Institute of Chemistry, Chinese Academy of Sciences, Beijing, People's Republic of China

Received: December 29, 2008; Revised Manuscript Received: February 16, 2009

Controllable aggregate transitions are achieved in this work by adding due amounts of β-cyclodextrin (β-CD) to mixed cationic/anionic surfactant aqueous solutions. In contrast to its "aggregate breaking" effect in single surfactant systems, aggregate growth is observed in nonstoichiometrical mixed cationic/anionic surfactant systems upon addition of β-CD. The aggregate growth typically undergoes a micellar elongation and a following micelle-to-vesicle transition, which in turn greatly influences the viscosity and absorbance of the solutions. A possible mechanism of this β-CD-induced aggregate growth is proposed. In mixed cationic/anionic surfactant systems, the surfactants strongly tend to reach electroneutral equilibrium in aggregates. In the present case, added β-CD is found to greatly facilitate the equilibrium by transferring the "major" component (whose molar fraction > 0.5) of a cationic/anionic surfactant mixture from the aggregates to β-CD cavities. Consequently, the surfactants in the aggregates approach electroneutral mixing, in favor of low-curved aggregates such as vesicles. This work shows that β-CD provides an additional degree of freedom to control microstructures and macroproperties for the whole class of mixed cationic/anionic surfactant systems.

Introduction

Amphiphilic molecules can self-assemble into various aggregates, such as micelles, vesicles, lamellae, and bicontinuous structures, in solutions.[1] Transitions between these aggregates are of particular interest, which stems from fundamental research and practical applications.[1] For example, micelle-to-vesicle transitions can be employed to load substances into the inner pool of the vesicles or to reconstitute membrane proteins into the vesicular membranes.[2] Aggregates that transform between symmetrical (e.g., spherical micelles and vesicles) and extremely unsymmetrical (e.g., elongated micelles) morphologies in response to temperature or light are promising building blocks for responsive viscoelastic fluids.[3] Vesicular transitions from isolated to densely packed states can cause phase separation,[4a,b] which may find applications in oil recovery and bioseparation.[4c−e] Moreover, aggregates with different morphologies can serve as templates for nanomaterial synthesis.[5] Therefore, tailoring aggregate morphologies in a controllable manner is highly desirable.

Recently, mixed cationic/anionic surfactant systems[6] have attracted increasing attention because of their advantages in synergism,[7] spontaneous formation of vesicles,[8] and aggregate polymorphism.[9] The above features, especially the aggregate polymorphism, greatly depend on the composition of cationic/anionic surfactants. In normal cationic/anionic surfactant systems, micelles, vesicles, and precipitates can be expected at surfactant compositions being far away from, close to, and exactly at the electroneutral mixing stoichiometry, respectively.[8] In a salt-free catanionic surfactant system, more interestingly, regular hollow icosahedra can be prepared with the anionic surfactant in slight excess, whereas flat nanodiscs are formed with the cationic surfactant in excess.[9a,b] Although several precedents realized aggregate transitions in this kind of systems by heating/cooling, varying pH, or adding salts, metal ions, or organic additives,[10] they are rather system-dependent and do not follow a general rule. Considering the deterministic effect of surfactant compositions on mixed cationic/anionic surfactant systems, we speculate that universal control over aggregate morphologies in such systems may be achieved by accessing the compositions.

Host−guest chemistry[11] does provide such a possibility. Cylcodextrins (CDs) are able to form host−guest complexes with most surfactants with high binding constants by including surfactants into CD cavities.[12] Because the outer surfaces of these cavities are hydrophilic, the resultant surfactant/CD complexes disfavor forming aggregates and are quite dissolvable in water.[12a] That is to say, CDs can remove surfactant molecules from aggregates. For single surfactant systems, the removal of surfactant molecules will break or "weaken" aggregates. For instance, adding β-CD can destroy micelles or the air/water interface adsorption layer[12a] and increase the fluidity and permeability of liposomes.[13] As to mixed surfactant systems, selective removal of one surfactant may occur. For example, β-CD prefers the fluorinated surfactant in a fluorinated /hydrogenated surfactant mixture due to size matching.[14] Thus, we assume that the selective removal in mixed cationic/anionic surfactant systems, if any, will benefit the direct adjustment of the surfactant compositions.

Herein, controllable aggregate transitions are realized by employing β-CD to directly adjust surfactant compositions in mixed cationic/anionic surfactant systems. Specifically, adding β-CD into nonstoichiometrical mixed cationic/anionic surfactant systems leads to progressive variations in microstructures and

* To whom correspondence should be addressed. Y.W.: e-mail, yilinwang@iccas.ac.cn; fax/telephone, 86-10-82615802. J.H.: e-mail, jbhuang@pku.edu.cn; fax, 86-10-62751708; telephone, 86-10-62753557.
[†] Peking University.
[‡] Chinese Academy of Sciences.

10.1021/jp811455f CCC: $40.75
Published on Web 03/23/2009

macroproperties of the systems: (1) aggregate growth that typically undergoes a micellar elongation and a following micelle-to-vesicle transition and (2) concomitant changes in viscosity and absorbance of the solutions. This β-CD-induced aggregate growth is attributed to the selective binding of β-CD to the "major" component (whose molar fraction > 0.5) of a cationic/anionic surfactant mixture. In virtue of the access to the surfactant composition, a key parameter in mixed cationic/anionic surfactant systems, β-CD features ubiquity of inducing aggregate growth for this kind of systems.

Experimental Section

Materials. Dodecyltriethylammonium bromide (DEAB) was prepared by reactions of 1-bromododecane with triethylamine, followed by recrystallizing five times from ethanol/acetone. ^{1}H NMR: δ 3.32 (q, 6H), 3.18 (t, 2H), 1.69 (m, 2H), 1.30 (m, 27H), 0.90 (t, 3H) ppm. Elementary analysis: found N 3.90%, C 60.95%, H 11.60%; calculated N 4.00%, C 61.70%, H 11.51%. Sodium dodecyl sulfate (SDS, 99%) was purchased from Acros Organics Co. and used as received. All the other used surfactants are of A. R. grade. The purity of the surfactants was testified by the absence of minimum in their surface tension curves. β-Cyclodextrin (β-CD) was purchased from Sinopharm Chemical Reagent Co. with a water content of 14%. For ^{1}H NMR measurements, we dehydrated β-CD powder by heating it before preparing its D_2O solution. Otherwise, β-CD was used without further treatment. D_2O (99.9%) was purchased from Cambridge Isotope Laboratories, Inc. Water (H_2O) was redistilled from potassium permanganate. Most experiments were done in the SDS/DEAB ($x_{SDS} = 0.8$, $C_T = 10$ mM) systems, where x_{SDS} and C_T are the molar fraction of SDS ($x_{SDS} + x_{DEAB} = 1$) and the total concentration of the surfactants, respectively.

Viscosity and Absorbance Measurements. Viscosities of solutions were measured using an Ubbelhode capillary viscometer with water as the reference at 25 °C. Absorbance measurements were carried out at 500 nm with a Beijing Purkinje General TU-1810 spectrophotometer whose temperature was controlled at 25 °C.

Freeze-Fracture Transmission Electron Microscopy (FF-TEM). Before the freezing procedure, samples were always incubated at 25 °C for more than 2 h. In the freezing procedure, a small amount of a sample was placed on a 0.1 mm thick copper disk and then covered with a second copper disk. The sample-loaded copper sandwich was frozen by plunging this sandwich into liquid propane which was cooled by liquid nitrogen. Aggregate structures were believed to be preserved and "solidified" by this procedure. Fracturing and replication were carried out in a freeze-fracture apparatus (BalzersBAF400, Germany) at −140 °C. Pt/C was deposited at an angle of 45° to shadow the replicas, and C was deposited at an angle of 90° to consolidate the replicas. The resulting replicas were examined in a JEM-100CX electron microscope.

Time-Resolved Fluorescence Quenching (TRFQ). The time dependent fluorescence intensity $I(t)$ of a probe in micelles in the presence of a quencher obeys the Infelta-Tachiya equation[15]

$$I(t) = I(0)\exp[-A_2 t - A_3(1 - \exp(-A_4 t))] \qquad (1)$$

where $I(0)$, A_2, A_3, and A_4 are the fluorescence intensity at $t = 0$, the unquenched fluorescence decay rate constant, the average number of quenchers per micelle, and the quenching rate constant, respectively. These parameters can be obtained by fitting fluorescence decay curves to eq 1 in a weighted least-squares procedure. Assuming monodisperse micelles, one can relate the aggregation number N_{agg} to A_3 by

$$N_{agg} = C^* A_3/[Q] \qquad (2)$$

where [Q] is the quencher concentration and C^* is the concentration of surfactant in micellar form.

In vesicles or other large aggregates, the decay curve is governed by the modified Stern−Volmer equation[15]

$$I(t) = I(0)\exp[-A_5 t - A_6 t^{1/2}] \qquad (3)$$

where A_5 is related to the Stern−Volmer parameter and A_6 is a "diffusion depletion" term.

In this work, pyrene was used as the fluorescence probe with dodecylpyridinium chloride (C_{12}PyCl) as the quencher. A desired amount of pyrene in ethanol was added to a test tube, followed by evaporation of the ethanol. Then a C_{12}PyCl-loaded DEAB/SDS/β-CD solution was added to the tube, which was vigorously stirred for 1 h. The concentration of pyrene was kept low enough (5×10^{-6} M) to prevent excimer formation. It has been shown in the literature that degassing neither affects the use of eq 1 in the main text nor provides a tangible gain in the fitting precision.[16] Therefore, samples were not subjected to degassing. Pyrene fluorescence decay curves were monitored by an Edinburgh FLS920 time-resolved fluorescence spectrophotometer (excitation at 337 nm and emission at 385 nm, at 25 °C). The fluorescence decay curves were fitted by the DECAN 1.0 software.

Dynamic Light Scattering (DLS). A commercialized spectrometer (Brookhaven Instruments Corporation, Holtsville, NY) equipped with a 100 mW solid-state laser (GXC-III, CNI, Changchun, China) operating at 532 nm was used to conduct dynamic light scattering experiments. Photon correlation measurements in self-beating mode were carried out at multiple

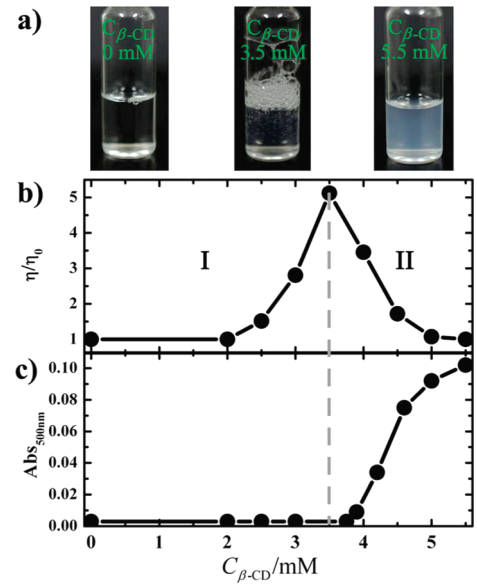

Figure 1. SDS/DEAB ($x_{SDS} = 0.8$, $C_T = 10$ mM) solutions with varied β-CD concentrations $C_{\beta\text{-CD}}$. (a) Photographs: left, $C_{\beta\text{-CD}} = 0$ mM, a transparent solution; middle, $C_{\beta\text{-CD}} = 3.5$ mM, a transparent solution that can trap bubbles for a moment; right, $C_{\beta\text{-CD}} = 5.5$ mM, a bluish solution. The variations of relative viscosity (b) and absorbance (c). The dashed line is a boundary of regions I and II.

scattering angles by using a BI-TurboCo Digital Correlator. The temperature was held at 25 °C by an external thermostat.

The normalized first-order electric field time correlation function $g^{(1)}(\tau)$ is related to the line width distribution $G(\Gamma)$ and the line width Γ by

$$g^{(1)}(\tau) = \int_0^\infty G(\Gamma) \exp(-\Gamma\tau)\, d\Gamma \quad (4)$$

By using a Laplace inversion program, CONTIN, the above equation can be solved to obtain $G(\Gamma)$ and Γ, where Γ is related to the diffusion coefficient D and the scattering vector q by $\Gamma = Dq^2$. The apparent hydrodynamic radius $R_{h,\,app}$ can be obtained according to the Stokes−Einstein equation

$$R_{h,app} = k_B T/(6\pi\eta D) \quad (5)$$

where k_B, T, and η are the Boltzmann constant, absolute temperature, and viscosity of the solvent, respectively.

^{1}H Nuclear Magnetic Resonance (^{1}H NMR). The ^{1}H NMR experiments were performed on a Bruker ARX 400 (^{1}H: 400.13 MHz) spectrometer with D_2O as solvent at 25.0 °C. Peaks of β-CD protons were denoted by COSY.

Results and Discussion

Aggregate Growth Induced by β-CD in a SDS-Rich SDS/DEAB ($x_{SDS} = 0.8$, $C_T = 10$ mM) System. Before addition of β-CD, the SDS/DEAB solution is transparent (Figure 1a, left) and of a water-like viscosity, indicating that the dominant aggregates are micelles. Upon addition of β-CD (0−3.5 mM, region I), the relative viscosity starts to rise at $C_{\beta\text{-CD}}$ (β-CD concentration in bulk solution) = 2 mM, and it reaches a maximum at $C_{\beta\text{-CD}} = 3.5$ mM (Figure 1b), while the absorbance (or optical density) remains unchanged (Figure 1c). The most viscous sample ($C_{\beta\text{-CD}} = 3.5$ mM) can trap bubbles for a moment (Figure 1a, middle). In region I, a micellar elongation may occur. since increased viscosity and low absorbance are typical characteristics for such an aggregate transition.[3] Further addition of β-CD (3.5−5.5 mM, region II) causes a decrease of the relative viscosity but an intense increase of the absorbance (Figure 1b and c). The solution with 5.5 mM β-CD has a bluish appearance, whereas its viscosity drops back to that of water (Figure 1a, right). The bluish color signals the presence of large particles or scatterers such as vesicles. In region II, a micelle-to-vesicle transition is thus possibly responsible for the above observation.

The morphologies of the proposed micelles and vesicles were examined by freeze-fracture transmission electron microscopy (FF-TEM). For the samples with 4.5 or 5.5 mM β-CD, vesicles with diameters ranging from 40 to 100 nm were readily verified (Figure 2a and b). For the samples with zero or low β-CD concentrations, the existence of vesicles is basically ruled out due to the lack of any vesicular structures in TEM observations, but micelles can hardly be visualized by this technique. Hence, we resorted to time-resolved fluorescence quenching (TRFQ) and dynamical light scattering (DLS) to further elucidate the microstructures in these samples.

In the TRFQ method, decay curves of a hydrophobic fluorescence probe in surfactant aggregates are recorded and then are fitted to appropriate equations. If the decay curve fits eq 1 well, the presence of micelles is suggested and the aggregation number N_{agg} of the micelles can be obtained by eq 2; if the decay curve fits eq 3 well, the existence of vesicles or other large aggregates is implied (see the Experimental Section for details). In region I ($C_{\beta\text{-CD}} = 0-3.5$ mM), the acquired decay curves fit eq 1 quite well. The N_{agg} value rises slightly from 328 to 479 and then sharply increases to 1220 upon β-CD addition (Figure 3a). This result demonstrates that micelles have grown to a large extent. Notably, the N_{agg} value of β-CD-free samples, 328, is much larger than that of spherical micelles (<100), implying a rodlike shape for the present micelles. The elongated micelles might be long enough to bring up a viscous increase, as illustrated in Figure 1b. In region II ($C_{\beta\text{-CD}}$ = 3.5−5.5 mM), the fitting of decay curves to eq 3 failed. This mismatch implies that some large self-assemblies, such as vesicles, other than micelles are presented. Quite expectedly, the fitting of these decay curves to eq 5 is successful, which confirms the existence of vesicles and agrees with the FF-TEM results (Figure 2).

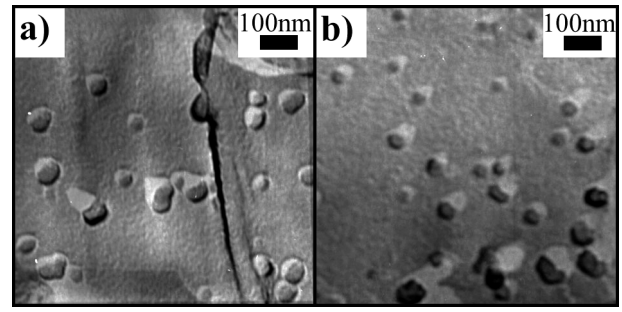

Figure 2. FF-TEM micrographs for SDS/DEAB ($x_{SDS} = 0.8$, C_T = 10 mM) solutions with $C_{\beta\text{-CD}} = 4.5$ mM (a) and 5.5 mM (b), respectively.

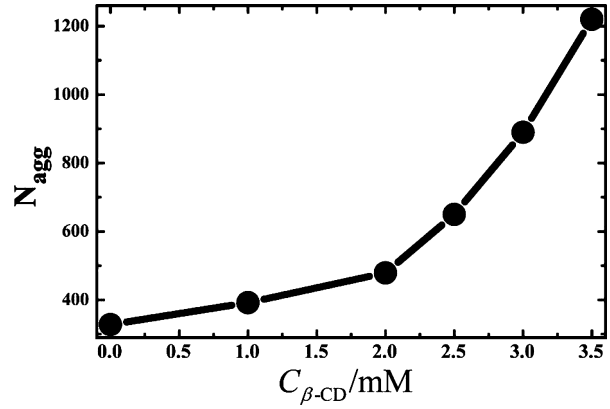

Figure 3. Variation of the micellar aggregation number N_{agg} upon adding different amounts of β-CD to the SDS/DEAB ($x_{SDS} = 0.8$, C_T = 10 mM) solution.

The laser light scattering method has been well established to noninvasively characterize particles in the range of ∼1−1000 nm. This method is employed to follow the aggregate growth in the present case. In Figure 4a, the scattering light intensity is plotted against $C_{\beta\text{-CD}}$ for the SDS/DEAB/β-CD solutions. The intensity goes through a steady and slight increase in region I and a sharp rise of near 30 times in region II, which is in accordance with the proposed micelle elongation in region I and the micelle-to-vesicle transition in region II. Qualitative particle size information can be retrieved by comparing autocorrelation curves, where large particles diffuse slowly and correspond to slowly decaying curves. In Figure 4b, samples with higher $C_{\beta\text{-CD}}$ exhibit slower decaying autocorrelation curves, suggesting larger particle sizes. Obvious distinctions between autocorrelation curves in regions I and II are recognizable, in line with the proposed two-stage aggregate growth model. To

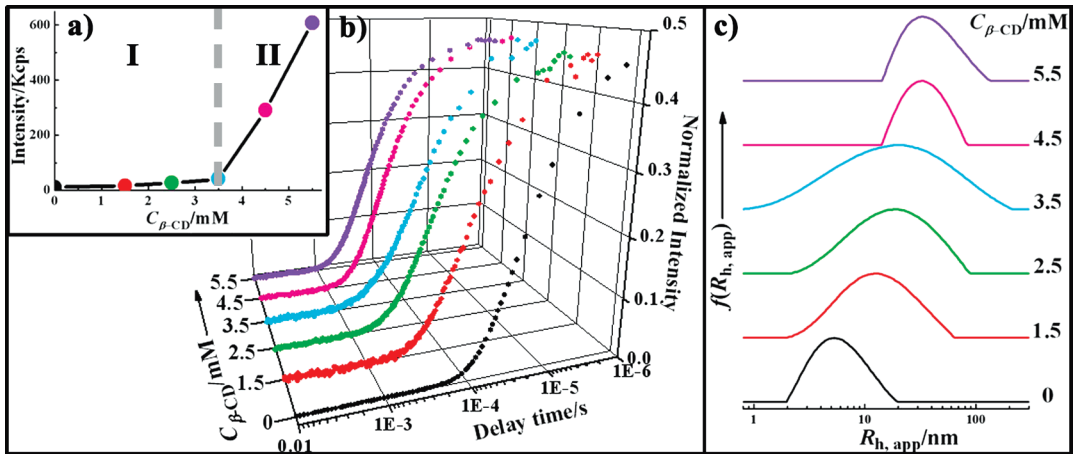

Figure 4. SDS/DEAB (x_{SDS} = 0.8, C_T = 10 mM) solutions with varied $C_{\beta\text{-CD}}$. Variations of the scattering light intensity (a), of autocorrelation curves (b), and of the apparent hydrodynamic radius $R_{h,app}$ as obtained by the CONTIN method (c), respectively. The dashed line in part a is a boundary of regions I and II.

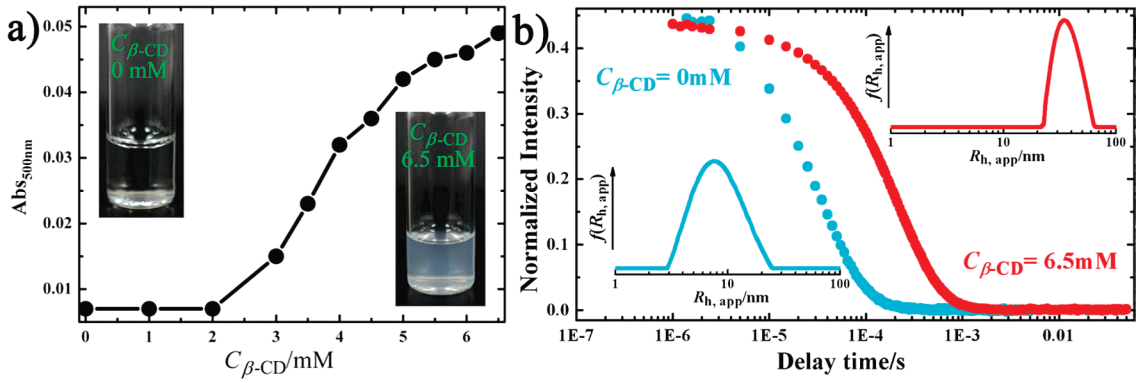

Figure 5. SDS/DEAB (x_{SDS} = 0.1, C_T = 10 mM) solutions with varied $C_{\beta\text{-CD}}$. (a) Solution absorbance versus $C_{\beta\text{-CD}}$. Insert photographs: left, $C_{\beta\text{-CD}}$ = 0 mM, a transparent solution; right, $C_{\beta\text{-CD}}$ = 6.5 mM, a bluish solution. (b) Autocorrelation curves and $R_{h,app}$ distributions for samples with $C_{\beta\text{-CD}}$ = 0 mM and 6.5 mM, respectively.

quantify the size variation, the autocorrelation curves were converted into distributions of the apparent hydrodynamic radius $R_{h,app}$ via the CONTIN method (Figure 4c). The addition of β-CD (up to 3.5 mM, region I) gradually shifts the $\langle R_{h,app}\rangle$ from 5.3 to 20 nm and broadens the size distribution. These $\langle R_{h,app}\rangle$ values fall in a typical range of rodlike micellar sizes, and the increased $\langle R_{h,app}\rangle$ confirms the micellar elongation. In addition, the samples with 2.5 and 3.5 mM β-CD display remarkable angular dependence (data not shown), corresponding to polydisperse rodlike micelles with high aspect ratios. In contrast, the plots in region II show a relatively narrow size distribution with a $\langle R_{h,app}\rangle$ of about 33 nm, which agrees with the dimension of near-spherical structures in FF-TEM micrographs (Figure 2). This result, together with the negligible angular dependence of the samples, suggests that most rodlike micelles have transformed into vesicles.

Combining the viscosity, absorbance, FF-TEM, TRFQ, and DLS results, we can draw a conclusion that, with the successive addition of β-CD to the SDS-rich SDS/DEAB (x_{SDS} = 0.8, C_T = 10 mM) solution, the original micelles elongate considerably and then transform into vesicles. Recently, it has been established that β-CD can form aggregates with diameters ∼ 200 nm above 3 mM by itself,[17] which might raise an argument about what are the observed aggregates in SDS/DEAB/β-CD solutions. The aggregates could be surfactant aggregates, β-CD aggregates, or both of them. To address this argument, control experiments were conducted in surfactant-free β-CD solutions (up to 10 mM β-CD, see Figures S1 and S2 in the Supporting Information). In absorbance (Figure S1a) and viscosity (Figure S1b) measurements, the absorbance and relative viscosity of the surfactant-free samples are always 0 and 1, respectively; that is, the samples are transparent and of a waterlike viscosity. These observations suggest that β-CD aggregates cannot result in pounced changes in macroproperties (absorbance and viscosity) of solutions as we observed in the case of SDS/DEAB/β-CD mixtures. In light scattering measurements (Figure S2), the intensity of each surfactant-free sample is significantly lower than that of the corresponding surfactant-loaded sample (less than 1/500), indicating that the number density of β-CD aggregates (if any) would be much less than that of surfactant aggregates in the case of SDS/DEAB/β-CD mixtures. Therefore, surfactant aggregates are predominant whereas β-CD aggregates are negligible in the present SDS/DEAB/β-CD solutions.

Universality of β-CD-Induced Aggregate Growth in Mixed Cationic/Anionic Surfactant Systems. This universality will be underlined by extending the scope of object surfactant systems from the studied SDS-rich SDS/DEAB system to (1) a DEAB-rich SDS/DEAB system, to (2) other SDS/DEAB systems with different ratios and concentrations, and to (3) other mixed cationic/anionic surfactant systems. Before β-CD addition, the appearance of a DEAB-rich SDS/DEAB (x_{SDS} = 0.1, C_T = 10 mM) solution is transparent (Figure 5a). DLS measurements in this solution revealed a fast decaying autocorrelation curve and a size distribution with $\langle R_{h,app}\rangle$ of 7 nm (Figure 5b), indicating that the major aggregates are micelles. The possibility for vesicles is basically excluded by TEM

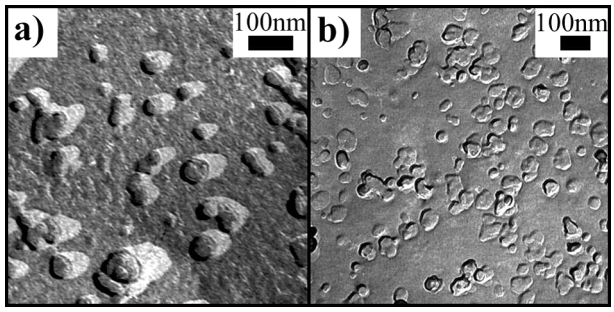

Figure 6. FF-TEM micrographs for the SDS/DEAB ($x_{SDS} = 0.1$, $C_T = 10$ mM) solution with 6.5 mM β-CD and for the SDS/DEAB ($x_{SDS} = 0.67$, $C_T = 10$ mM) solution with 2 mM β-CD, respectively.

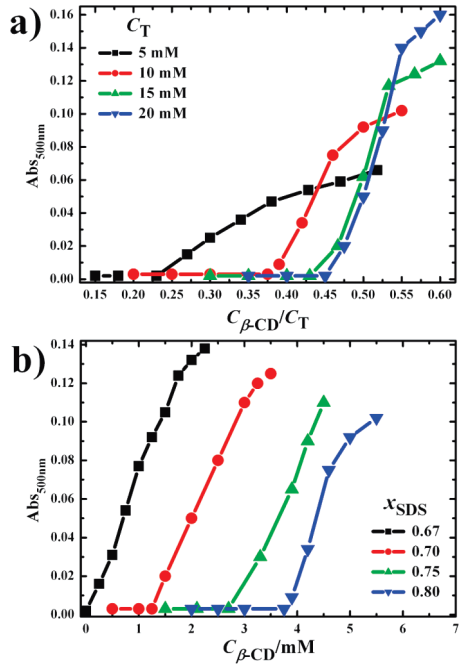

Figure 7. Variation of the solution absorbance with the addition of β-CD in different SDS/DEAB systems: (a) x_{SDS} is constant at 0.8, and C_T is varied. (b) C_T is constant at 10 mM, and x_{SDS} is varied.

observations. Upon the addition of β-CD, the solution absorbance rises progressively (Figure 5a). The sample with 6.5 mM β-CD shows a bluish appearance (Figure 5a), which is a sign of a vesicular solution. The existence of vesicles was verified by a slow decaying autocorrelation curve and a corresponding size distribution with $\langle R_{h,app} \rangle$ of 35 nm in Figure 5b, as well as by vesicular structures with diameters ranging from 30 to 100 nm in Figure 6a. Clearly, the addition of β-CD to this DEAB-rich system leads to a micelle-to-vesicle transition.

Effects of the total surfactant concentration (C_T) and surfactant composition (x_{SDS}) on the β-CD-induced aggregate growth are demonstrated in Figure 7. In Figure 7a, the absorbance is plotted against the ratio $C_{\beta\text{-CD}}/C_T$, where x_{SDS} is constant at 0.8 and C_T varies from 5 to 20 mM. With the increase of C_T, the maximum absorbance increases, and the onset ratio for absorbance to increase shifts to a higher value. In Figure 7b, the absorbance is plotted against $C_{\beta\text{-CD}}$, where x_{SDS} varies from 0.67 to 0.8 and C_T is constant at 10 mM. With x_{SDS} getting apart from 0.5, the maximum absorbance decreases, and the onset $C_{\beta\text{-CD}}$ for absorbance to increase shifts to a higher value. These results suggest that added β-CD induces micelle-to-vesicle transitions in the above SDS/DEAB systems. FF-TEM observations confirmed the existence of vesicles in the samples with desired $C_{\beta\text{-CD}}$. Figure 6b shows a representative micrograph for a SDS/DEAB ($x_{SDS} = 0.67$, $C_T = 10$ mM) solution with 2 mM β-CD, where plenty of 30−80 nm structures can be observed. The universality of the β-CD-induced aggregate growth is now corroborated for nonstoichiometrical SDS/DEAB systems.

Furthermore, the β-CD-induced aggregate growth was generally identified for a board range of mixed nonstoichiometrical cationic/anionic surfactant systems, where cationic surfactants cover C_nTA^+, C_nEA^+, and C_nPy^+, and anionic surfactants cover C_nS^-, $C_nSO_3^-$, and $C_nCO_2^-$.[18] In most cases, micellar elongations and/or micelle-to-vesicle transitions are observed. In some cases, micellar or vesicular growth followed by precipitation or phase separation occurs, which depends on the nature of a specific cationic/anionic surfactant mixture. Anyway, these results suggest that β-CD can be employed as a universal and effective additive to fine-tune aggregates or microstructures for the whole class of mixed cationic/anionic surfactant systems.

Mechanism of This β-CD-Induced Aggregate Growth. The addition of β-CD was traditionally believed to weaken or destroy surfactant aggregates; however, it is found here that the addition of β-CD to the nonstoichiometrical cationic/anionic surfactant systems induces the aggregate growth. As mentioned in the Introduction, aggregates in β-CD-free mixed cationic/anionic surfactant systems transform from micelles via vesicles to precipitations (i.e., a growth process) due to a decrease of aggregate surface charge density when the surfactant compositions get close to elctroneutral mixing. This fact gives us a hint that, in the present cases, the added β-CD may selectively form inclusion complexes with the major component of a cationic/anionic surfactant mixture, removing it from the aggregates; such removal leaves the composition in the aggregates approaching an electroneutral mixing stoichiometry, leading to the observed aggregate growth. To prove this proposal, we conducted nuclear magnetic resonance (NMR) and fluorescence quenching experiments to examine the formation of surfactant/β-CD complexes and the variation of aggregate surface charge density, respectively.

Representative ^{1}H NMR results of SDS/DEAB/β-CD systems are shown in Figure 8, where remarkable differences can be noted in the spectra of β-CD in the presence (Figure 8a) and absence (Figure 8b) of surfactants. In line with formation of surfactant/β-CD complexes, H_3 and H_5 of β-CD, both of which locate at the inner surface of the cavity, exhibit a significant upfield shift upon surfactant addition. Moreover, the observed chemical shift (δ) can quantify the molar fraction of complexed β-CD, $x^c_{\beta\text{-CD}}$ (its counterpart is free or uncomplexed β-CD, i.e., $x^c_{\beta\text{-CD}} + x^f_{\beta\text{-CD}} = 1$) by

$$\delta = x^c_{\beta\text{-CD}}\delta^c + x^f_{\beta\text{-CD}}\delta^f \text{ or equivalently } \Delta\delta = \delta - \delta^f = x^c_{\beta\text{-CD}}(\delta^c - \delta^f) \quad (6)$$

where δ^f and δ^c are the proton chemical shifts of free and complexed β-CD, respectively. These two values of H_5 are determined by Job's plots of SDS/β-CD (Figure 8c) and DEAB/β-CD (not shown, similar to the former) complexes, leading to[14a]

$$\Delta\delta(H_5) = -0.175x^c_{\beta\text{-CD}} \quad (7)$$

Obviously, subjecting $\Delta\delta(H_5)$ values of SDS/DEAB/β-CD samples to eq 7 yields $x^c_{\beta\text{-CD}}$ values (Figure 8d). It is found that, in all the samples ($C_{\beta\text{-CD}} = 1-5$ mM), most β-CD molecules

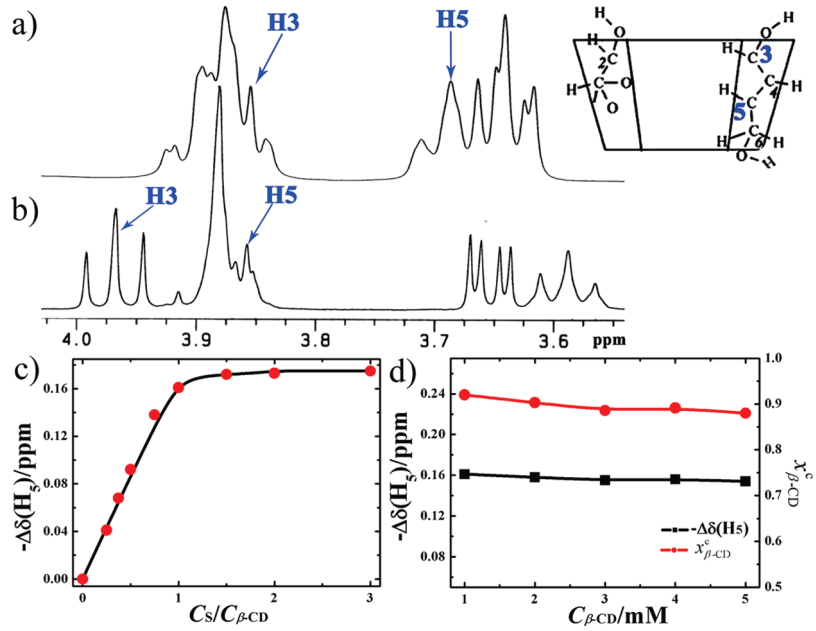

Figure 8. ^{1}H NMR spectra of β-CD (3 mM) in the absence (a) and presence (b) of SDS/DEAB ($x_{SDS} = 0.8$, $C_T = 10$ mM); the solvent is D_2O. The inner graph is the molecular structure of β-CD, where H_3 and H_5 are highlighted. (c) Chemical shifts of β-CD's H_5 versus surfactant/β-CD concentration ratios. The closed circles are experimental data, where the surfactant is SDS alone, $C_{β\text{-CD}}$ is constant at 5 mM, and C_S is varied. The solid line is fitted by assuming a 1:1 binding model and $K_b = 2.45 \times 10^4$ M^{-1}. (d) Chemical shifts of β-CD's H_5 (closed squares) or molar fraction of complexed β-CD ($x^c_{β\text{-CD}}$, closed circles) versus $C_{β\text{-CD}}$ in SDS/DEAB ($x_{SDS} = 0.8$, $C_T = 10$ mM) solutions.

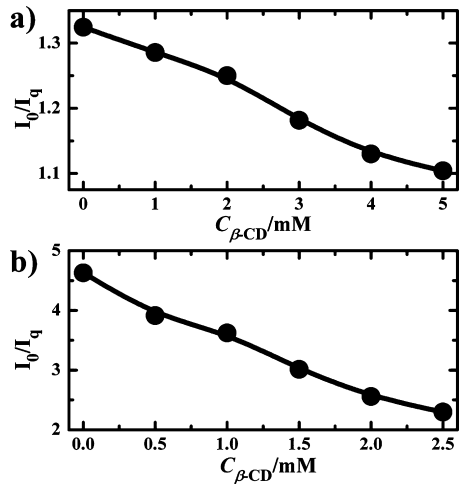

Figure 9. Variations of quenching efficiency I_0/I_q with the addition of β-CD to a SDS/DEAB ($x_{SDS} = 0.8$, $C_T = 10$ mM) solution (a) and to a SDS/DEAB ($x_{SDS} = 0.1$, $C_T = 10$ mM) solution (b).

SCHEME 1: Aggregate Growth in Mixed Cationic/Anionic Surfactant Systems Induced by β-CDa

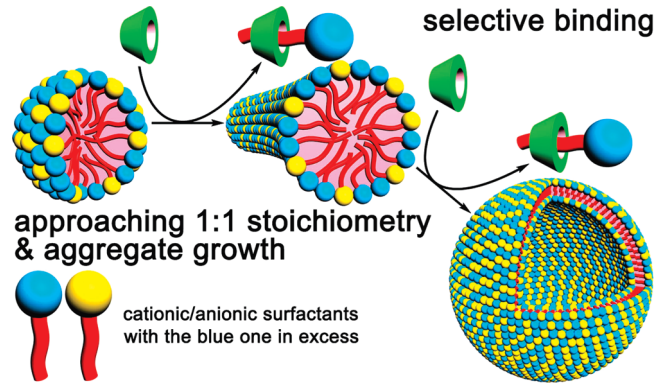

[a] For surfactant/β-CD inclusion complexes, mutual orientations of the surfactant and β-CD are uncertain.

(~90%) are in a complexed state. Thus, the formation of surfactant/β-CD complexes is confirmed, although the selectivity of β-CD to SDS or DEAB is still not clear.

A decrease of aggregate surface charge density with addition of β-CD to SDS/DEAB solutions was detected by fluorescence quenching experiments. In the presence of hydrophilic quenchers such as Cs^+ and $S_2O_3^{2-}$, the fluorescence intensities of pyrene in aggregates depend on the local concentrations of quenchers in the palisade and electrical double layers of aggregates. For charged aggregates, the local concentration of the oppositely charged quenchers ascends with the increase of aggregate surface charge density. Therefore, the quenching efficiencies (i.e., the ratio of fluorescence intensity without and with the quencher, I_0/I_q) of Cs^+ or $S_2O_3^{2-}$ to pyrene reflect the surface charge densities of the aggregates. As shown in Figure 9, the quenching efficiency descends with the addition of β-CD in a SDS-rich and a DEAB-rich system, confirming that the aggregate surface charge density is lowered by the addition of β-CD.

The above NMR and fluorescence quenching experiments support our proposal that a part of the major surfactant is removed from the aggregates to β-CD cavities upon β-CD addition. This mechanism of the β-CD-induced aggregate growth is illustrated in Scheme 1. The origin of the selectivity of β-CD to the major component can be understood as follows. Clearly, nonstoichiometrical mixed cationic/anionic surfactant aggregates are of a net surface charge, which will electrostatically attract the minor surfactant with a countercharge and will electrostatically repel the major surfactant with a cocharge. That is to say, the surfactants strongly tend to reach electroneutral equilibrium in aggregates. In the present case, added β-CD greatly facilitates the equilibrium by transferring the major surfactant from the aggregates to β-CD cavities.

Conclusion

Cationic/anionic surfactant/β-CD ternary aqueous systems are systematically investigated, where this work focuses on the effect of β-CD addition on aggregate morphologies and solution properties. It is found that β-CD can profoundly affect the systems at two levels. Microscopically, it controls aggregates, including spherical micelles, rodlike micelles (and their length), vesicles, and precipitates. The observed aggregate growth as induced by β-CD contradicts the well-accepted "aggregate breaking" effect of β-CD and may advance understanding of surfactant/CD interactions. Macroscopically, it alters solution properties such as viscosity, absorbance, and phase separation. As to the origin of these influences, the selective binding of β-CD toward the major component of a cationic/anionic surfactant mixture is thought to be responsible: this selectivity removes the excess part of the major component from the aggregates, shifts the surfactant compositions in the aggregates toward an electroneutral mixing stoichiometry, and thus gives rise to the observed aggregate growth and concomitant variations in solution properties. As a result of the access to the surfactant composition, a key parameter in mixed cationic/anionic surfactant systems, β-CD features ubiquity of inducing aggregate growth for the whole class of mixed oppositely charged surfactant systems. In addition, the present aggregate-control strategy is based on host−guest interactions where no covalent or permanent change is imported, suggesting that the influences of β-CD may be undone by using another strong guest to compete the host. We hope the present work can open a new vista to fine-tune microstructures and macroproperties in self-assembling systems.

Acknowledgment. This work was supported by the National Natural Science Foundation of China (20873001, 20633010, and 50821061) and the National Basic Research Program of China (Grant No. 2007CB936201). We would like to thank the Center for Biological Electron Microscopy, the Institute of Biophysics for electron microscopy work, and Shufeng Sun for making TEM samples.

Supporting Information Available: Figures S1 and S2, showing the relative viscosity and absorbance versus $C_{\beta\text{-CD}}$ and the scattering intensity versus $C_{\beta\text{-CD}}$. This information is available free of charge via the Internet at http://pubs.acs.org.

References and Notes

(1) (a) Evans, D. F.; Wennerstrom, H. *The Colloidal Domain*; Wiley-VCH: New York, 2001. (b) Fendler, J. *Membrane Mimetic Chemistry*; John Wiley & Sons: New York, 1983. (c) Shaul, B.; Gelbart, W. M.; Roux, D. *Micelles, Membranes, Microemulsions and Monolayers*; Springer: Berlin, 1995.

(2) (a) Reeves, P. J.; Hwa, J.; Khorana, H. G. *Proc. Natl. Acad. Sci. U.S.A.* **1999**, *96*, 1927. (b) McQuade, D. T.; Quinn, M. A.; Yu, S. M.; Polans, A. S.; Krebs, M. P.; Gellman, S. H. *Angew. Chem., Int. Ed.* **2000**, *39*, 758. (c) Seddon, A. M.; Curnow, P.; Booth, P. J. *Biochim. Biophys. Acta* **2004**, *1666*, 105.

(3) (a) Davies, T. S.; Ketner, A. M.; Raghavan, S. R. *J. Am. Chem. Soc.* **2006**, *128*, 6669. (b) Ketner, A. M.; Kumar, R.; Davies, T. S.; Elder, P. W.; Raghavan, S. R. *J. Am. Chem. Soc.* **2007**, *129*, 1553.

(4) (a) Wang, K.; Yin, H. Q.; Sha, W.; Huang, J. B.; Fu, H. L. *J. Phys. Chem. B* **2007**, *111*, 12997. (b) Yin, H. Q.; Huang, J. B.; Mao, M.; Fu, H. L. *Langmuir* **2002**, *18*, 9198. (c) Narayanan, J.; Deotare, V. W. *Phys. Rev. E* **1999**, *60*, 4597. (d) Piazza, R.; Pierno, M.; Vignati, E. *Phys. Rev. Lett.* **2003**, *90*, 208101. (e) Vesperinas, A.; Eastoe, J.; Wyatt, P.; Grillo, I.; Heenan, R. K.; Richards, J. M.; Bell, G. A. *J. Am. Chem. Soc.* **2006**, *128*, 1468.

(5) (a) Yin, H. Q.; Lei, S.; Zhu, S. B.; Huang, J. B.; Ye, J. P. *Chem.—Eur. J.* **2006**, *12*, 2825. (b) Hentze, H.-P.; Raghavan, S. R.; McKelvey, C. A.; Kaler, E. W. *Langmuir* **2003**, *10*, 1069.

(6) For reviews, see: (a) Hao, J.; Hoffmann, H. *Curr. Opin. Colloid Interface Sci.* **2004**, *9*, 279. (b) Tondre, C.; Caillet, C. *Adv. Colloid Interface Sci.* **2001**, *93*, 115. Note that a similar term "catanionic surfactant" refers to a compound that is usually formed by an equimolar chemical reaction of a basic and an acidic surfactant. For example, see: (c) Consola, S.; Blanzat, M.; Perez, E.; Garrigues, J. C.; Bordat, P.; Rico-Lattes, I. *Chem.—Eur. J.* **2007**, *13*, 3039. (d) Rico-Lattes, I.; Blanzat, M.; Franceschi-Messant, S.; Perez, E.; Lattes, A. *C. R. Chim.* **2005**, *8*, 807.

(7) (a) Rosen, M. J. *Surfactants and Interfacial Phenomena*; Wiley & Sons: New York, 1989. (b) Yu, Z. J.; Zhao, G. X. *J. Colloid Interface Sci.* **1989**, *130*, 414.

(8) (a) Kaler, E. W.; Murthy, A. K.; Rodriguez, B. E.; Zasadzinski, J. A. N. *Science* **1989**, *245*, 1371. (b) Kaler, E. W.; Herrington, K. L.; Murthy, A. K.; Zasadzinski, J. A. N. *J. Phys. Chem.* **1992**, *96*, 6698.

(9) For icosahedra, see: (a) Dubios, M.; Deme, B.; Gulik-Krzywicki, T.; Dedieu, J.-C.; Vautrin, C.; Desert, S.; Perez, E.; Zemb, T. *Nature (London)* **2001**, *411*, 672. For flat nanodiscs, see: (b) Zemb, T.; Dubios, M.; Deme, B.; Gulik-Krzywicki, T. *Science* **1999**, *283*, 816. For onion structures, see: (c) Song, A. X.; Dong, S. L.; Jia, X. F.; Hao, J. C.; Liu, W. M.; Liu, T. B. *Angew. Chem., Int. Ed.* **2005**, *44*, 4018. For polyhedra, see: (d) Gonzalez-Perez, A.; Schmutz, M.; Waton, G.; Romero, M. J.; Krafft, M. P. *J. Am. Chem. Soc.* **2007**, *129*, 756. For tubelike structures, see: (e) Lu, T.; Han, F.; Li, Z. C.; Huang, J. B.; Fu, H. L. *Langmuir* **2006**, *22*, 2045. and. (f) Yan, Y.; Xiong, W.; Li, X. X.; Lu, T.; Huang, J. B.; Li, Z. C.; Fu, H. L. *J. Phys. Chem. B* **2007**, *111*, 2225. For hollow cones, see: (g) Douliez, J.-P. *J. Am. Chem. Soc.* **2005**, *127*, 15694.

(10) (a) Yin, H. Q.; Zhou, Z. K.; Huang, J. B.; Zheng, R.; Zhang, Y. Y. *Angew. Chem., Int. Ed.* **2003**, *42*, 2188. (b) Renoncourt, A.; Vlachy, N.; Bauduin, P.; Drechsler, M.; Touraud, D.; Verbavatz, J. M.; Dubois, M.; Kunz, W.; Ninham, B. W. *Langmuir* **2007**, *23*, 2376. (c) Hao, J. C.; Wang, J. Z.; Liu, W. M.; Adbel-Rahem, R.; Hoffmann, H. *J. Phys. Chem. B* **2004**, *106*, 3335. (d) Song, A. X.; Jia, X. F.; Teng, M. M.; Hao, J. C. *Chem.—Eur. J.* **2007**, *13*, 496. (e) Mao, M.; Huang, J. B.; Zhu, B. Y.; Ye, J. P. *J. Phys. Chem. B* **2002**, *106*, 219. (f) Jiang, L. X.; Wang, K.; Deng, M. L.; Wang, Y. L.; Huang, J. B. *Langmuir* **2008**, *24*, 4600.

(11) (a) Pedersen, C. J. *J. Am. Chem. Soc.* **1967**, *89*, 2495. (b) Pedersen, C. J. *Angew. Chem., Int. Ed. Engl.* **1988**, *27*, 1021.

(12) (a) Saenger, W.; Muller-Fahrnow, A. *Angew. Chem., Int. Ed. Engl.* **1988**, *27*, 393. (b) Junquera, E.; Tardajos, G.; Aicart, E. *Langmuir* **1993**, *9*, 1213. (c) Mwakibete, H.; Cristantino, R.; Bloor, D. M.; Wyn-Jones, E.; Holzwarth, J. F. *Langmuir* **1995**, *11*, 57. (d) Dorrego, A. B.; Garcia-Rio, L.; Herves, P.; Leis, J. R.; Mejuto, J. C.; Perez-Juste, J. *Angew. Chem., Int. Ed.* **2000**, *39*, 2945. (e) Park, J. W.; Song, H. J. *J. Phys. Chem.* **1989**, *93*, 6454. (f) Dharmawardana, U. R.; Christian, S. D.; Tucker, E. E.; Taylor, R. W.; Scamehorn, J. F. *Langmuir* **1993**, *9*, 2258.

(13) (a) Nishijo, J.; Shiota, S.; Mazima, K.; Inoue, Y.; Mizuno, H.; Yoshida, J. *Chem. Pharm. Bull.* **2000**, *48*, 48. (b) Puglisi, G.; Fresta, M.; Ventura, C. A. *J. Colloid Interface Sci.* **1996**, *180*, 542.

(14) (a) Xing, H.; Lin, S. S.; Yan, P.; Xiao, J. X.; Chen, Y. M. *J. Phys. Chem.* **2007**, *111*, 8089. (b) Patil, S. R.; Turmine, M.; Peyre, V.; Durand, G.; Pucci, B. *Talanta* **2007**, *74*, 72.

(15) (a) Almgren, M.; Lofroth, J. E. *J. Colloid Interface Sci.* **1981**, *81*, 486. (b) Tachiya, M. *Chem. Phys. Lett.* **1975**, *33*, 289. (c) Almgren, M. *Adv. Colloid Interface Sci.* **1992**, *41*, 9.

(16) Singh, J.; Unlu, Z.; Ranganathan, R.; Griffiths, P. *J. Phys. Chem. B* **2008**, *112*, 3997.

(17) (a) Bonini, M.; Rossi, S.; Karlsson, G.; Almgren, M.; Nostro, P. L.; Baglioni, P. *Langmuir* **2006**, *22*, 1478. (b) Rossi, S.; Bonini, M.; Nostro, P. L.; Baglioni, P. *Langmuir* **2007**, *23*, 10959, and references therein.

(18) Abbreviations: C_nTA^+, alkyl trimethyl ammonium; C_nEA^+, alkyl triethyl ammonium; C_nPy^+, alkyl pyridinium; C_nS^-, alkyl sulfate; $C_nSO_3^-$, alkyl sulfonate; $C_nCO_2^-$, alkyl carboxylate.

JP811455F